

1 **Urea-Nonstoichiometric Co-modulated LaMnO₃ for Ultra-High**
2 **Gaseous Hg⁰ Uptake Across a Broad Temperature Range**

3 Runlong Hao^{a,b,1}, Zhen Qian^{a,b,1}, Xiaomeng Zuo^a, Peng Qin^a, Xiaojie Yang^a, Zhao Ma^{a,b}, Bo Yuan^{*,a,b}

4 ^a *Hebei Key Lab of Power Plant Flue Gas Multi-Pollutants Control, Department of Environmental Science
5 and Engineering, North China Electric Power University, Baoding, 071003, PR China.*

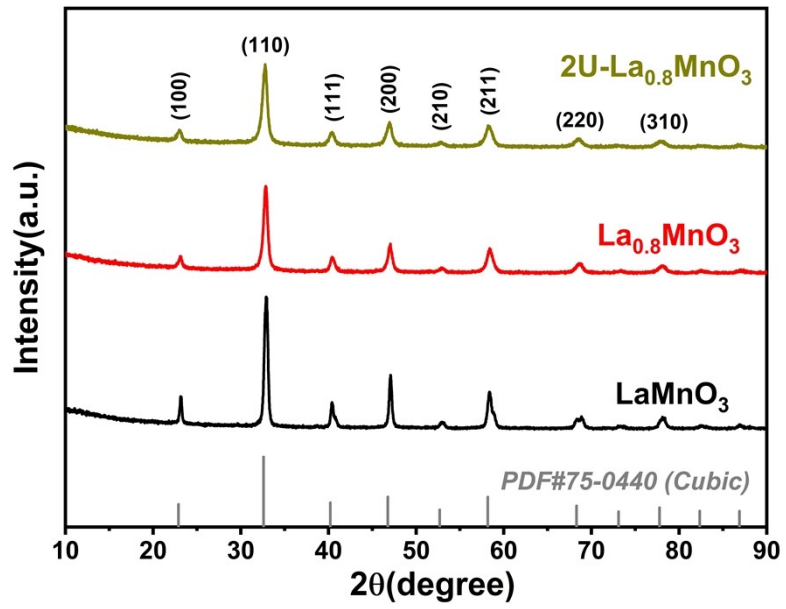
6 ^b *MOE Key Laboratory of Resources and Environmental Systems Optimization, College of Environmental
7 Science and Engineering, North China Electric Power University, Beijing, 102206, PR China.*

8 *Corresponding authors E-mail: hnyuanbo0407@163.com.

9 ¹Co-first author.

10 Text S1. Reagents and Materials

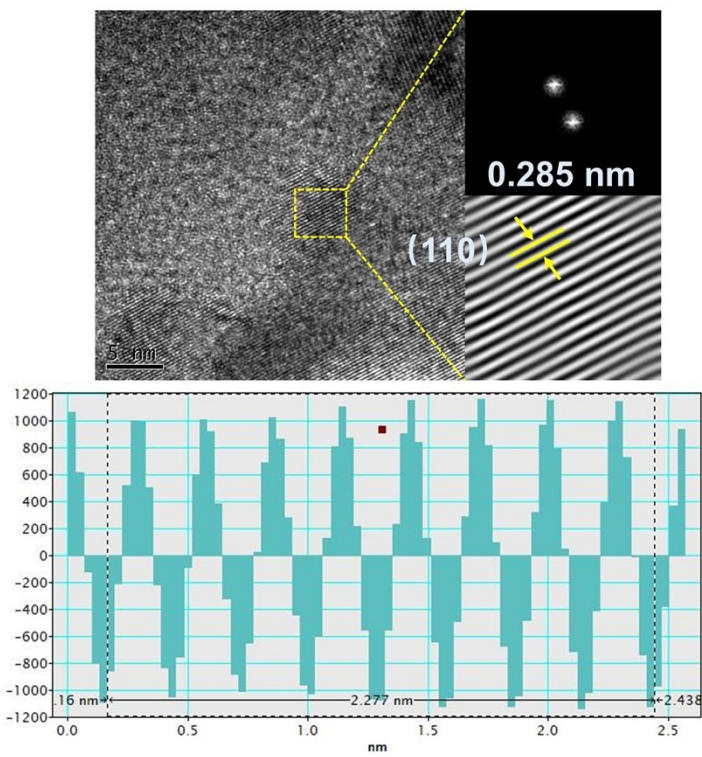
11 All reagents are of analytical grade, purchased from Macklin and Aladdin Reagent Malls (Shanghai,
12 China). Lanthanum nitrate hexahydrate ($\text{La}(\text{NO}_3)_3 \cdot 6\text{H}_2\text{O}$, 99%), manganese nitrate solution ($\text{Mn}(\text{NO}_3)_2$, 50
13 wt%) citric acid ($\text{C}_6\text{H}_8\text{O}_7 \cdot \text{H}_2\text{O}$, 99.5%) and urea ($\text{CH}_4\text{N}_2\text{O}$, 99%) are used for the perovskite synthesis. 0.5
14 mol/L stannous chloride (SnCl_2 , 99%) was utilized to confirm whether Hg^{2+} was existed in tail gas. 4 wt%
15 potassium permanganate (KMnO_4 , 99%) and 10% v/v sulfuric acid (H_2SO_4 , 95-98%) were used to capture
16 the Hg^0 in tail gas.



17

18

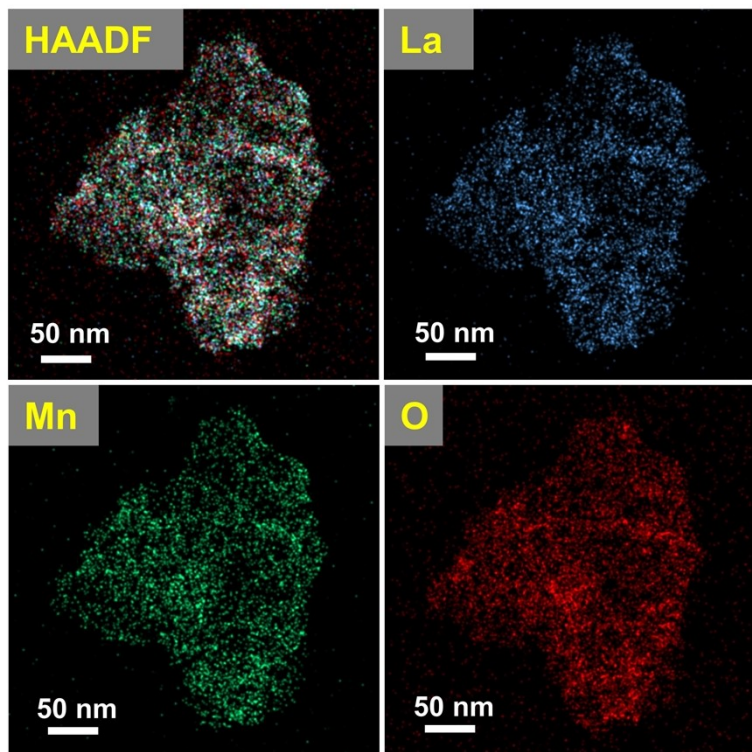
Fig. S1. XRD patterns of LaMnO₃, La_{0.8}MnO₃ and 2U-La_{0.8}MnO₃.



19

20

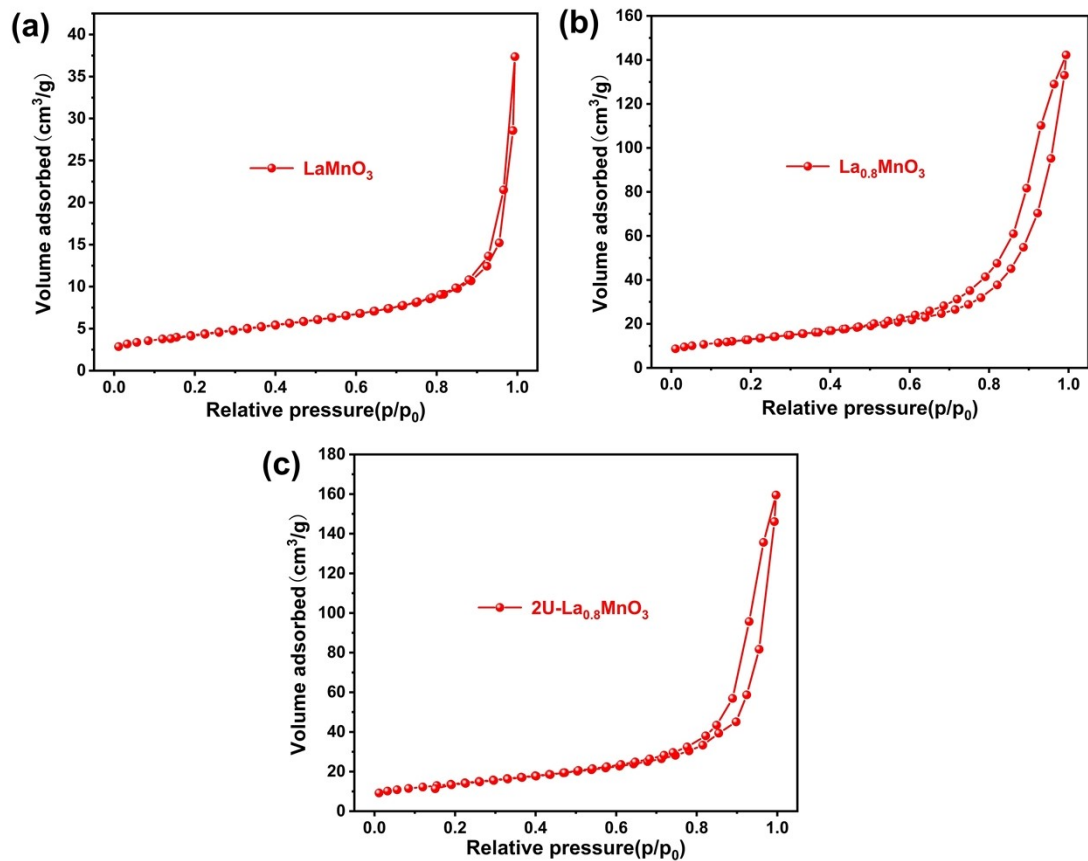
Fig. S2. HRTEM images of 2U-La_{0.8}MnO₃.



21

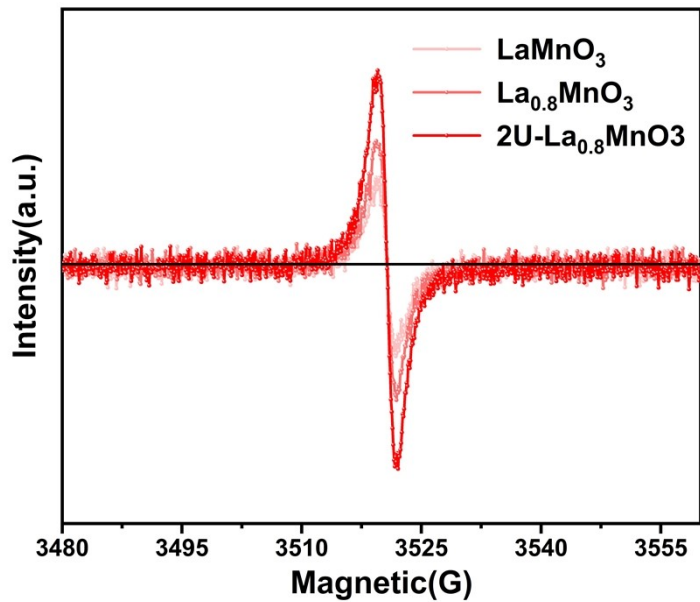
22

Fig. S3. EDX element mapping images of $2\text{U}-\text{La}_{0.8}\text{MnO}_3$.



23

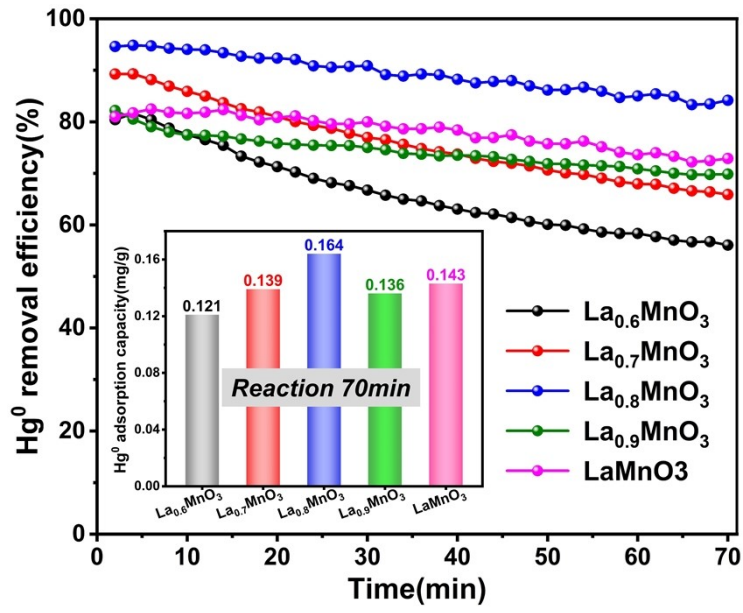
24 **Fig. S4.** The nitrogen adsorption-desorption isotherms of LaMnO_3 , $\text{La}_{0.8}\text{MnO}_3$ and $2\text{U-La}_{0.8}\text{MnO}_3$.



25

26

Fig. S5. EPR spectra of LaMnO_3 , $\text{La}_{0.8}\text{MnO}_3$ and $2\text{U}-\text{La}_{0.8}\text{MnO}_3$.



27

28 **Fig. S6.** The Hg^0 removal efficiency of $\text{La}_{1-x}\text{MnO}_3$ ($x= 0, 0.1, 0.2, 0.3, 0.4$), and the inset indicate the
29 dynamic adsorption capacity when the Hg^0 breakthrough reached 5%.

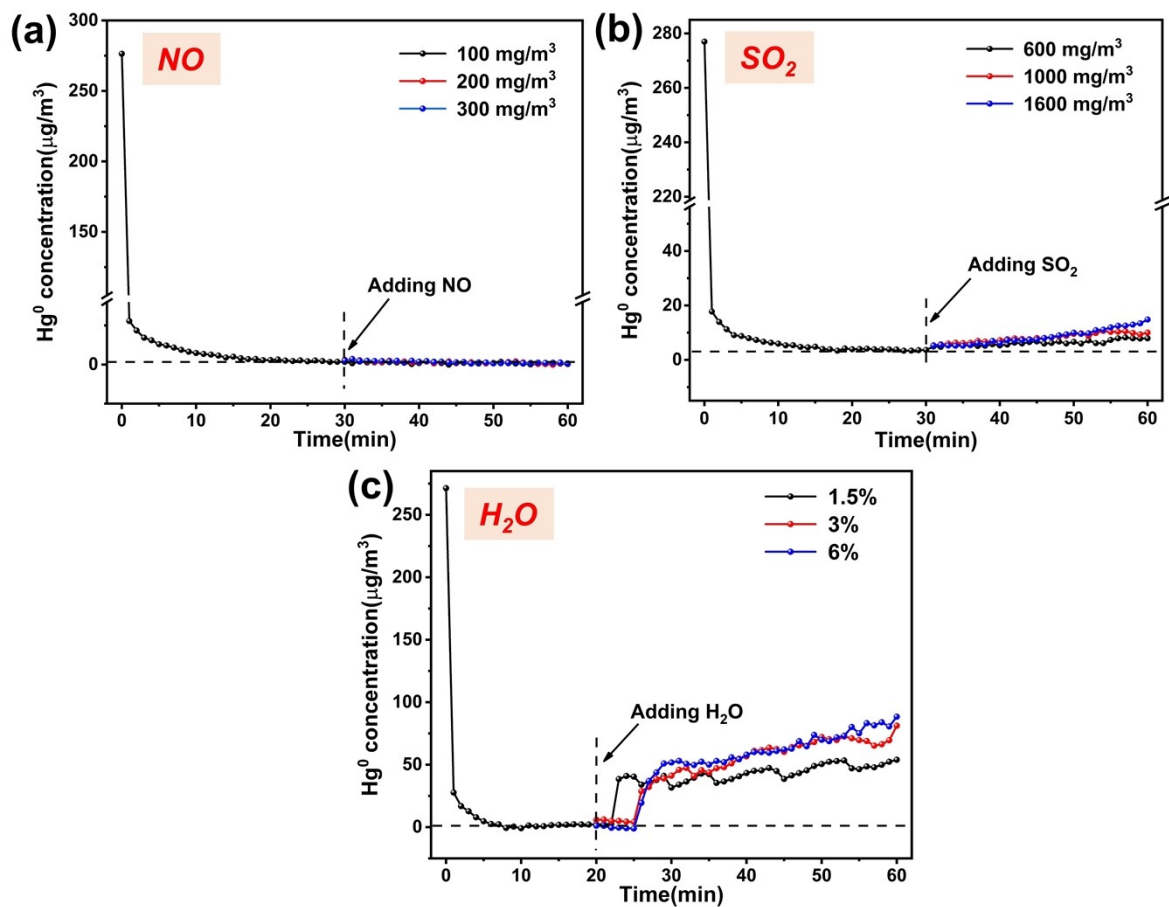
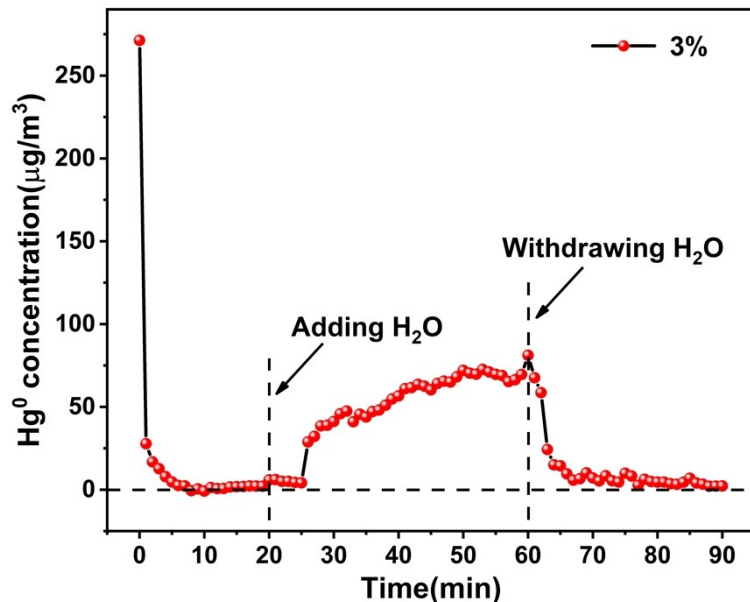


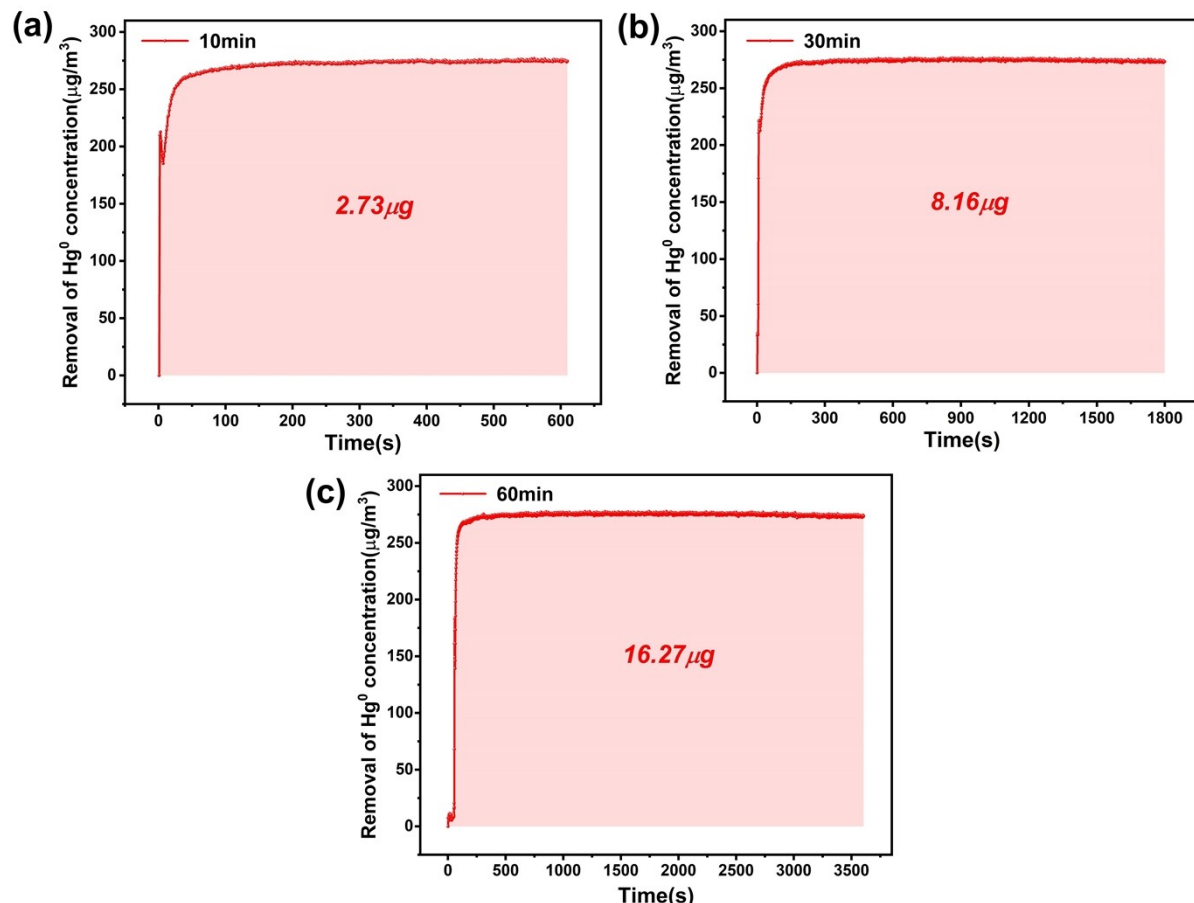
Fig. S7. Influences of (a)NO, (b)SO₂ and (c)H₂O on the Hg⁰ removal efficiency.



33

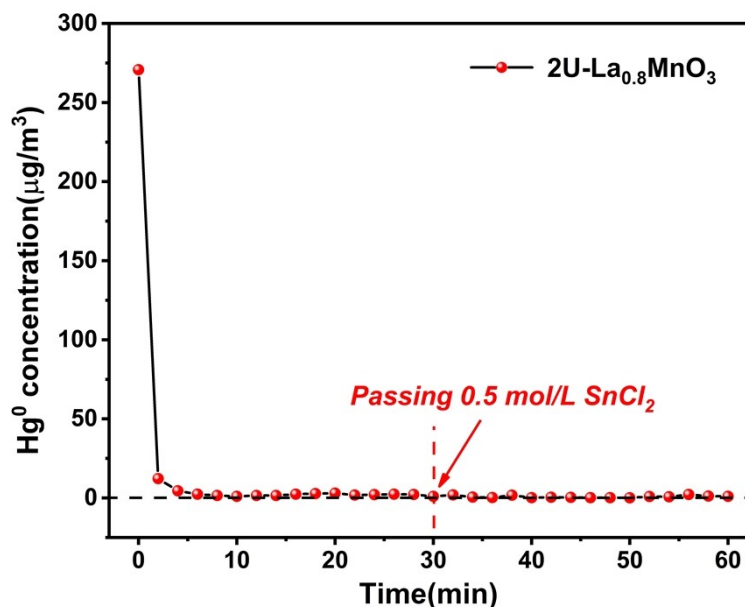
34

Fig. S8. The dynamic influence of H₂O on the Hg⁰ removal efficiency.



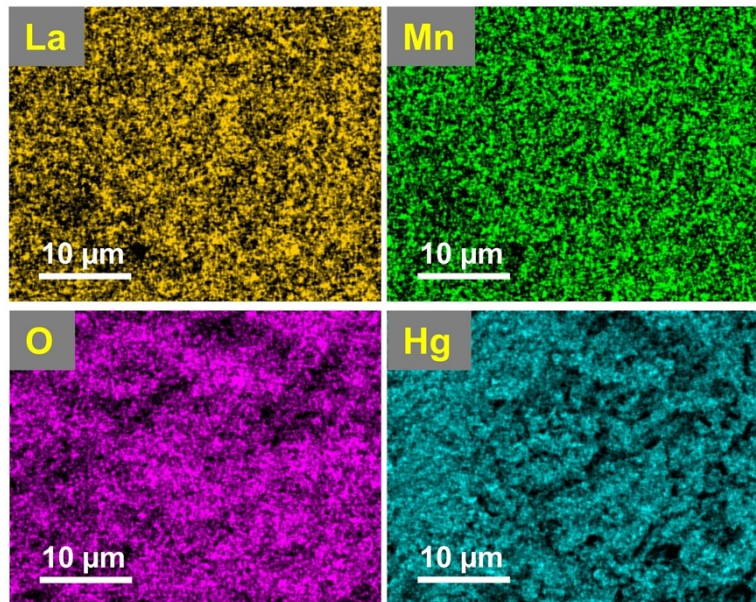
35

36 **Fig. S9.** Experimental calculation of Hg^0 released after reaction for (a) 10, (b) 30 and (c) 60 min.



37

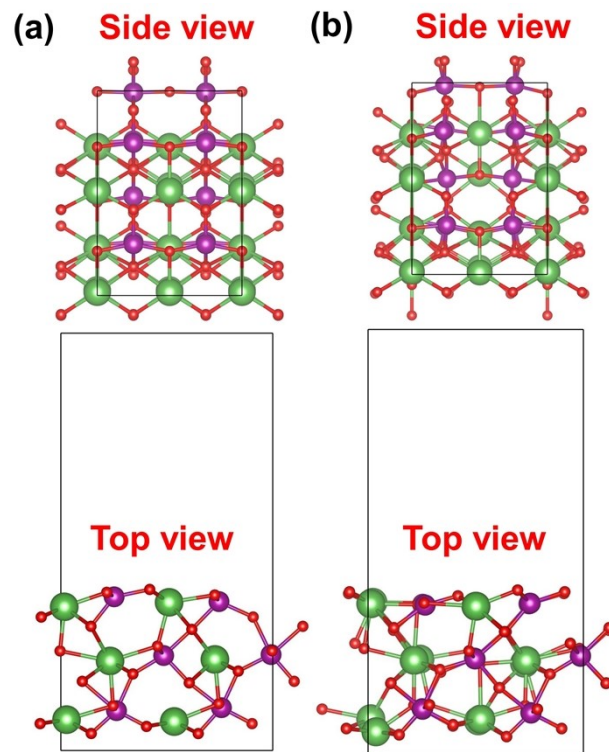
38 **Fig. S10.** The Hg⁰ removal performance with and without SnCl₂ solution.



39

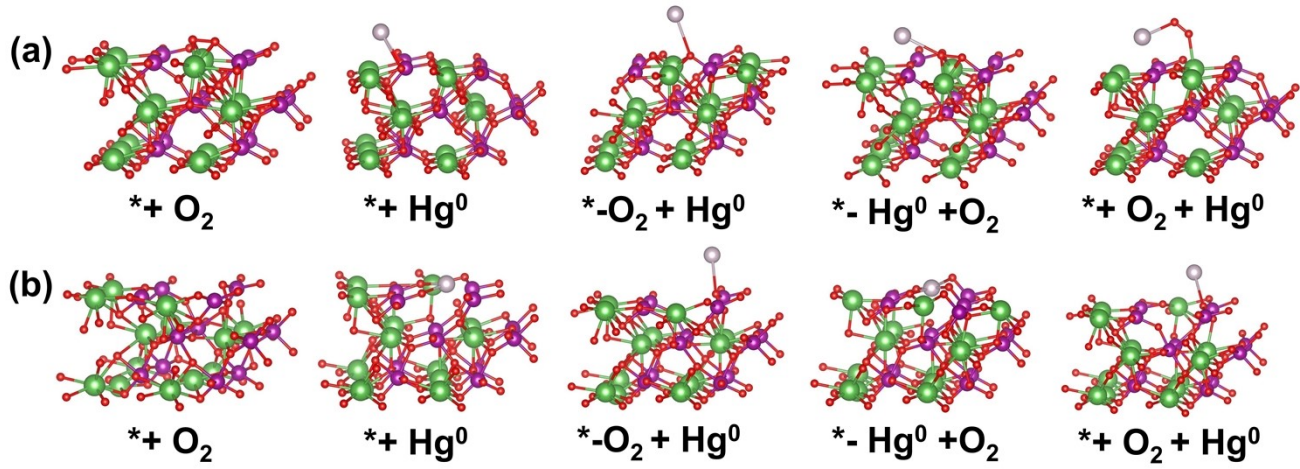
40

Fig. S11. EDX element mapping images of spent 2U-La_{0.8}MnO₃.



41

42 **Fig. S12.** Calculated side and top view configurations of (a) LaMnO₃ and (b) 2U-La_{0.8}MnO₃.



43

44 **Fig. S13.** The configurations of O₂ and Hg⁰ on (a) LaMnO₃ and (b) 2U-La_{0.8}MnO₃ (110) surface (*).

45 **Table S1.** The comparison of the Hg⁰ adsorption capacity of 2U-La_{0.8}MnO₃ with other oxides

Oxides	Temperatur e	Removal efficiency	Hg ⁰ Adsorption capacity (mg/g)	Breakthrough ratio/adsorption time	References
2U-La _{0.8} MnO ₃	40 ~ 250	100%	23.86	100%	This work
Mn/ γ -Fe ₂ O ₃	200	-	3.54	55%	1
(Fe ₂ Ti) _{0.8} O ₄	250	-	3.94	23%	2
α -MnO ₂	150	92%	6.94	10 h	3
LaMnO ₃	150	-	7.65	100%	4
CeO ₂ /TiO ₂	200 ~ 250	> 90%	0.012	4 h	5
Fe ₃ O _{4-x} Se _y	100	100%	8.80	100%	6
MoS ₃ /TiO ₂	100	-	14.90	75%	7
La _{0.8} Ce _{0.2} MnO ₃	50 ~ 200	> 80%	5.83	30 h	8
Fe ₂ O ₃ /TiO ₂	50 ~ 150	> 95%	2.69	10 h	9
CeO ₂ -CrO _x	50 ~ 100	100%	0.168	6.7 h	10
α -Fe ₂ O ₃ /SnO ₂	400	99%	4.84	2 h	11
LaFeO ₃	40 ~ 160	> 80%	2.397	1 h	12
Ce-Pd/ γ -Al ₂ O ₃	250	> 98%	0.038	4.2 h	13

46 References

- 47 (1) Yang, S.; Guo, Y.; Yan, N.; Qu, Z.; Xie, J.; Yang, C.; Jia, J. Capture of Gaseous Elemental Mercury
48 from Flue Gas Using a Magnetic and Sulfur Poisoning Resistant Sorbent Mn/ γ -Fe₂O₃ at Lower
49 Temperatures. *J. Hazard. Mater.* **2011**, *186*, 508-515.
- 50 (2) Yang, S.; Guo, Y.; Yan, N.; Wu, D.; He, H.; Qu, Z.; Yang, C.; Zhou, Q.; Jia, J. Nanosized Cation-
51 deficient Fe-Ti spinel: a Novel Magnetic Sorbent for Elemental Mercury Capture from Flue Gas. *ACS Appl.*
52 *Mater. Interfaces*. **2011**, *3*, 209-217.
- 53 (3) Xu, H.; Qu, Z.; Zhao, S.; Mei, J.; Quan, F.; Yan, N. Different Crystal-forms of One-dimensional MnO₂
54 Nanomaterials for the Catalytic Oxidation and Adsorption of Elemental Mercury. *J. Hazard. Mater.* **2015**,
55 *299*, 86-93.
- 56 (4) Xu, H.; Qu, Z.; Zong, C.; Quan, F.; Mei, J.; Yan, N. Catalytic Oxidation and Adsorption of Hg⁰ over
57 Low-temperature NH₃-SCR LaMnO₃ Perovskite Oxide from Flue Gas. *Appl. Catal., B* **2016**, *186*, 30-40.
- 58 (5) Li, H.; Wu, C.; Li, Y.; Zhang, J. CeO₂-TiO₂ Catalysts for Catalytic Oxidation of Elemental Mercury in
59 Low-rank Coal Combustion Flue Gas. *Environ. Sci. Technol.* **2011**, *45*, 7394-7400.
- 60 (6) Yang, Z.; Li, H.; Yang, Q.; Qu, W.; Zhao, J.; Feng, Y.; Hu, Y.; Yang, J.; Shih, K. Development of
61 Selenized Magnetite (Fe₃O_{4-x}Se_y) as an Efficient and Recyclable Trap for Elemental Mercury Sequestration
62 from Coal Combustion Flue Gas. *Chem. Eng. J.* **2020**, *394*, 125022.
- 63 (7) Mei, J.; Wang, C.; Kong, L.; Liu, X.; Hu, Q.; Zhao, H.; Yang, S. Outstanding Performance of Recyclable
64 Amorphous MoS₃ Supported on TiO₂ for Capturing High Concentrations of Gaseous Elemental Mercury:
65 Mechanism, Kinetics, and Application. *Environ. Sci. Technol.* **2019**, *53*, 4480-4489.
- 66 (8) Yang, J.; Na, Y.; Hu, Y.; Zhu, P.; Meng, F.; Guo, Q.; Yang, Z.; Qu, W.; Li, H. Granulation of Mn-based
67 Perovskite Adsorbent for Cyclic Hg⁰ Capture from Coal Combustion Flue Gas. *Chem. Eng. J.* **2023**, *459*,
68 141679.

- 69 (9) Xing, X.; Zhang, X.; Tang, J.; Cui, L.; Dong, Y. Removal of Gaseous Elemental Mercury from
70 Simulated Syngas over $\text{Fe}_2\text{O}_3/\text{TiO}_2$ Sorbents. *Fuel* **2022**, *311*, 122614.
- 71 (10) Ye, D.; Wang, X.; Wang, R.; Hu, Y.; Liu, X.; Liu, H. Relationship between Hg^0 Capture Performance
72 and Physicochemical Properties of $\text{CeO}_2\text{-CrO}_x$ Mixed Oxides. *J. Environ. Chem. Eng.* **2022**, *10*, 108252.
- 73 (11) Ma, Y.; Xu, T.; Li, L.; Wang, J.; Li, Y.; Zhang, H. Core-shell Nanostructure $\alpha\text{-Fe}_2\text{O}_3/\text{SnO}_2$ Binary
74 Oxides for the Catalytic Oxidation and Adsorption of Elemental Mercury from Flue Gas. *J. Environ. Chem.
75 Eng.* **2021**, *9*, 105137.
- 76 (12) Pei, H.; Li, X.; Song, Y.; Zhang, M.; Wang, D.; Wu, J.; Wang, F.; Zhang, Y.; Zhao, X.; Jia, T. LaFeO_3
77 Perovskite Nanoparticles for Efficient Capture of Elemental Mercury from Coal-fired Flue Gas. *Fuel* **2022**,
78 *309*, 122134.
- 79 (13) Huo, Q.; Yue, C.; Wang, Y.; Han, L.; Wang, J.; Chen, S.; Bao, W.; Chang, L.; Xie, K. Effect of
80 Impregnation Sequence of $\text{Pd/Ce}/\gamma\text{-Al}_2\text{O}_3$ Sorbents on Hg^0 Removal from Coal Derived Fuel Gas.
81 *Chemosphere*. **2020**, *249*, 126164.